

Rapid Note

Coexistence of antiferromagnetic and ferromagnetic phase for ferromagnetic Kondo lattice model

H. Yi^{1,a}, J. Yu², and S.-I. Lee^{1,3}¹ National Creative Research Initiative Center for Superconductivity, Pohang University of Science and Technology, Pohang 790-784, Korea² Department of Physics, Sogang University, Seoul 121-742, Korea³ Department of Physics, Pohang University of Science and Technology, Pohang 790-784, Korea

Received: 1st September 1998 / Revised: 30 October 1998 / Accepted: 27 November 1998

Abstract. To study the proposed phase separations in doped manganites, we performed Monte-Carlo calculations for the ferromagnetic Kondo lattice model with strong Hund's coupling between conduction electrons and localized spins. For the practical calculations, we adopted a one dimensional lattice and treated the spins of the localized t_{2g} electrons semi-classically. A direct evidence of the phase separation is observed from a snapshot of the spatial dependence of localized spins. No indication of the canted or spiral phases is found in the results of simulations. Further, the calculated results of the spin structure factor in the phase separation region are well compared with recent experiments.

PACS. 75.30.-m Intrinsic properties of magnetically ordered materials – 75.30.Et Exchange and superexchange interactions – 71.10.-w Theories and models of many electron systems

The colossal magnetoresistance in doped perovskite lanthanum manganites such as $\text{La}_{1-x}(\text{Sr,Ca})_x\text{MnO}_3$ has attracted great interest due to its possible technological applications [1]. These materials reveal peculiar behavior in the phase diagram where the antiferromagnetic (AF) phase is associated with insulating properties and the ferromagnetic (FM) phase with metallic properties as well as charge ordering [2]. For a broad range of doping, $0.2 \lesssim x \lesssim 0.5$, the correlation between FM moments and metallic conductivity can be well understood in terms of the double exchange mechanism [3,4]. However, for a small hole doping range of $0 \lesssim x \lesssim 0.2$, the nature of the magnetic structure is still controversial. In particular, several neutron scattering [5,6] and NMR [7] experiments revealed coexisting AF and FM diffraction peaks, which had been interpreted as an appearance of the weak homogeneous canted FM phase. Recently, however, there are contradictory experimental results reported [8–11]. Especially, one NMR observation [10] showed the evidence of FM and AF micro-domains but not the canted phase. This phase separation (PS) has been an important issue in many strongly correlated systems. One of such examples is in high- T_c superconductors [12]. So far there is no theoretical report on the spin arrangements in the PS region,

even though it is essential to understand the ground state nature of small doped manganites.

A stable canted AF phase was predicted theoretically by de Gennes [4] based on a molecular approximation of a combined model of double exchange and AF superexchange interactions. Another view, *i.e.*, the existence of the predicted PS was also reported theoretically by Nagaev [13] and Arovas *et al.* [14] in the context of the Schwinger boson formalism. Kagan *et al.* [15] also raised a question about the stability of the canted phase in a quantum version of the double exchange model. The existence of PS in the FM Kondo lattice model for the doped manganite systems was first addressed by Yunoki and coworkers [16]. In the following works by Yunoki and Moreo [17] and by us [18], the antiferromagnetic superexchange interactions between localized spins in the FM Kondo lattice model were found to be crucial in understanding the phase separation. In spite of such intensive research efforts, however, it is still desired to have a detailed comparison of theoretical predictions with experimental observations on the magnetic properties of lightly doped manganites.

In this paper, we report the results of our Monte-Carlo studies on the phase separation region near $x \approx 0$ of the FM Kondo lattice model for the lightly doped manganites. In contrast to the previous approach [16–18], we have attempted to identify the phase separation through the density of state analysis while varying the chemical

^a e-mail: hsyi@anyon.postech.ac.kr

potentials and snapshots of the localized t_{2g} spins. In order to extract information on the real-space distribution of the localized spins, we calculated the number of nodes as well as spin-spin correlation functions in order to clarify the issue of the canted phase *versus* the spiral states and PS. The snapshots of localized spins clearly indicate the evidence of the PS, but not the canted phase. Although we considered primarily the one-dimensional lattice model in this work, the PS regions were shown to exist in higher dimensions [17,18]. When the evolution of the magnetic correlations only is concerned, our results can be considered to be at least qualitatively a representative of the high dimensional case. Further, our analysis of the calculated results are consistent with the results of neutron diffraction experiment [6].

The FM Kondo model Hamiltonian including a strong Hund's coupling term as well as a hopping term is written by

$$H = -\sum_{\langle ij \rangle \sigma}^L \left(t_{ij} c_{i\sigma}^+ c_{j\sigma} + \text{h.c.} \right) - J_H \sum_{iab}^L \mathbf{S}_i \cdot \boldsymbol{\sigma}_{ab} c_{ia}^+ c_{ib}, \quad (1)$$

where $\boldsymbol{\sigma}_{ab}$ is the Pauli matrix for the conduction electron spins and the \mathbf{S}_i represents the localized spin of t_{2g} electrons. This Hamiltonian is popularly adopted for the description of the doped magnates for doping level of $0.2 \lesssim x \lesssim 0.5$. The operator $c_{i\sigma}$ ($c_{i\sigma}^+$) annihilates (creates) a conduction electron with spin index σ and the site index i . The first term represents an effective hopping of e_g conduction electrons between the nearest-neighbor Mn sites. The second term is a FM Hund's coupling between e_g conduction electrons and localized spins of t_{2g} electrons. L is the system size. Within a semi-classical treatment of the t_{2g} spins, the trace over the e_g electrons in the partition function could be carried out exactly. The integration over the localized spins was performed using a standard Metropolis algorithm. Calculations were performed for the 1D chain with $L = 24$. Only nearest neighborhood hopping was considered. The parameters used for the calculations were $t_{ij} = t$, $J_H = 12t$ and $T = t/80$. Unless stated otherwise, we take $t = 1$, $J_H = 12t$, $T = t/80$ and $L = 24$. Periodic boundary conditions in spatial directions were used. For a given chemical potential μ , the density was determined as a result of simulations. In actual calculations, typically 6×10^4 initial sequences of configurations were discarded for the thermalization processes before real data were collected. We actually took 2×10^5 data for each measurement depending on numerical accuracies.

The PS at a certain doping level could be characterized by a drastic change of the density of states $N(\omega)$ with a small change of μ . The lower band of $N(\omega)$ is presented for various values of μ at $J_H = 8$ and $T = 1/120$ in Figure 1. The broken line at $\omega - \mu = 0$ indicates Fermi energy E_F [19]. For $\mu \gtrsim -6.6907$, the system is almost insulating because E_F lie in the edge of the lower band. As μ decrease further, the nature of $N(\omega)$ change drastically indicating the crossover between insulating and metallic states. For $\mu \lesssim -6.6910$, the system is metallic because the lower bands run across the Fermi energy. In this region, the bandwidth is equal to about 4 which is close

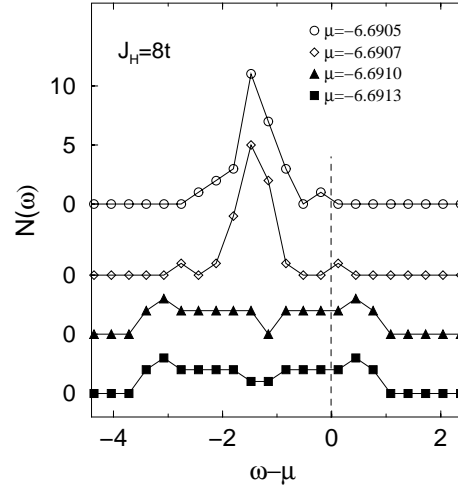


Fig. 1. Density of states $N(\omega)$ as a function of energy for various values of μ at $J_H = 8$ and $T = 1/120$.

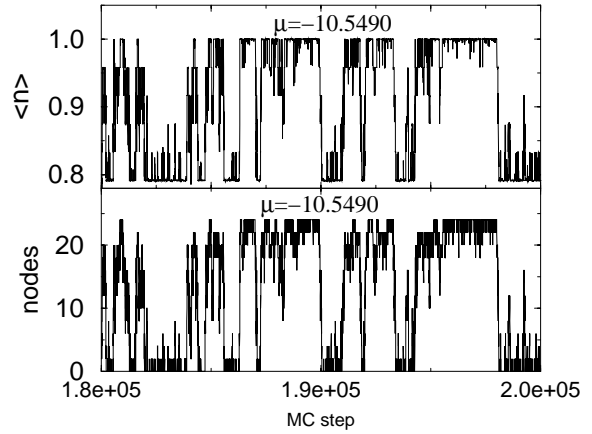


Fig. 2. (a) The density of itinerant electrons $\langle n \rangle$ as a function of the Monte-Carlo steps for an $L = 24$ chain with $J_H = 12t$, $T = t/80$ and $\mu = -10.5490$. (b) Number of node for localized spin S_z .

to the one from the dispersion relation in 1-dimensional double exchange model. However, the bandwidth change abruptly near critical $\mu \approx -6.6910$. This discontinuity of bandwidth imply the phase instability, *i.e.*, PS of the system.

In our results, the PS is clearly observed in a range of band filling near $x \approx 0$, which is consistent with the previous work [16–18]. Systems within the PS region become unstable and the density fluctuates as a function of Monte-Carlo steps. Figure 2a shows the time evolution of the density of the itinerant electrons for a critical chemical potential $\mu = -10.5490$. Wild fluctuations in the density are observed with frequent jumps between two stable phases of $\langle n \rangle = 1.0$ and $\langle n \rangle = 0.79$. This is an intrinsic characteristic of the PS. To understand this behavior in detail, we calculated the magnetic correlations, *i.e.*, the configurations of the localized spins. Figure 2b shows the number of nodes of the localized spin S_z as a function of Monte-Carlo step. For a FM spin configuration, the number

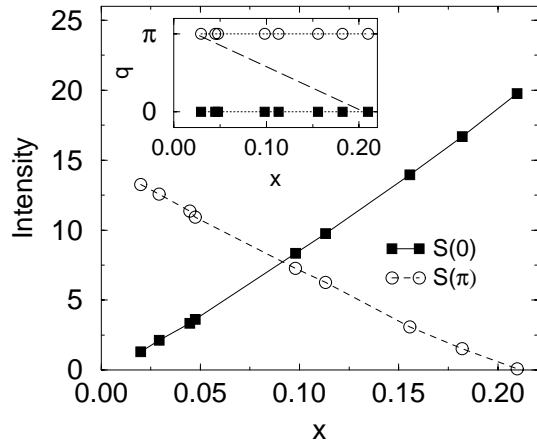


Fig. 3. Doping dependence of the FM and AF peak intensity of structure factor for $J_H = 12t$ and $T = t/80$. The dominant component crosses over from the AF to FM component around $x \sim 0.09$.

of nodes is zero while for an AF spin configuration the number of nodes is L . As indicated in Figure 2, this number for S^z and the density $\langle n \rangle$ is closely related. An AF phase is dominant near $\langle n \rangle \approx 1$ while the FM phase is dominant near $\langle n \rangle \approx 0.79$. The admixture of the AF and FM component is the origin of a spatial phase separation between hole-poor AF and hole-rich FM region.

To probe the spin-spin correlations in the PS region, we calculated the spin structure factor $S(q)$ as defined by

$$S(\mathbf{q}) = (1/L) \sum_{\mathbf{l}, \mathbf{m}} e^{i(1-\mathbf{m}) \cdot \mathbf{q}} \langle \mathbf{S}_{\mathbf{l}} \cdot \mathbf{S}_{\mathbf{m}} \rangle. \quad (2)$$

Shown in Figure 3 are the peak intensities of the spin structure factor $S(q)$ for the range of $0 \lesssim x \lesssim 0.22$. In this region, $S(q)$ has a two-peak structure, one at the AF q -vector, *i.e.*, $q = \pi$ and the other at the FM q -vector, *i.e.*, $q = 0$. Near $x \sim 0.09$, there is a crossover between the AF and FM components. This gradual crossover is associated with an additive nature of $S(q)$ for the two phases. Care must be taken in analyzing the $S(q)$ since two peaks could also show up in the canted phase which is characterized by a single phase with two sub-lattice magnetization one having a nonzero value [13]. For example, Kawano *et al.* [6] interpreted the observed two-peak structure as a weak canted ferromagnetism. Usually the distinction between the phase separation and the canted phase requires the presence of an applied magnetic field [4,5,13]. But, in this case, snapshots of spin configuration could clearly indicate that the two-peak structure is related to the PS, not to the canted ferromagnetism.

The two-peak structure of $S(q)$ does not discern the PS or the canted phase, but clearly rules out the recent claim of the spiral structure proposed by Inoue and Maekawa [20] based on the Hubbard FM Kondo lattice model with AF superexchange interaction (J_{AF}) between localized spins in the strong U limit. If the spin structure $S(q)$ changes continuously from $q = \pi$ to $q = 0$ with the increase of x , the locus of q should follow the dashed line as shown in inset of Figure 3. But, this is not the

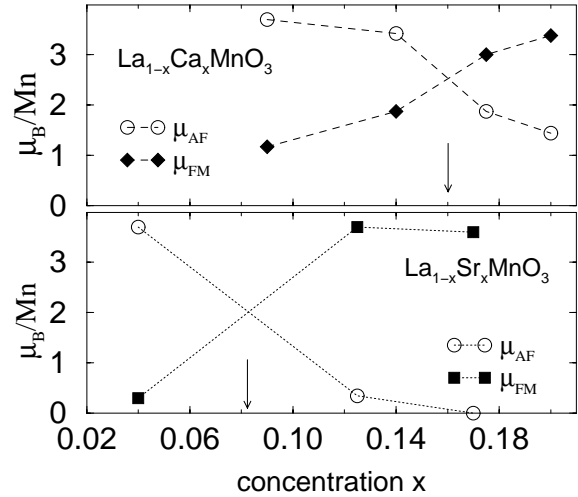


Fig. 4. (a) FM and AF moments as a function of tetra-valent manganese (Mn^{4+}) from reference [5], and (b) from reference [6].

case in the results in this work. Maybe such contradictory results could have originated from J_{AF} . Although small in its magnitude, J_{AF} seem to play a crucial role in the magnetic properties of $\text{La}_{1-x}(\text{Sr}, \text{Ca})_x\text{MnO}_3$. Indeed, our preliminary study [21] indicates that the FM ordering temperature T_c is very sensitive to small J_{AF} variations for $x \sim 0.3$.

For a comparison of our results in $S(q)$ with experiments, we plotted the changes of magnetic moments in $\text{La}_{1-x}\text{Ca}_x\text{MnO}_3$ and $\text{La}_{1-x}\text{Sr}_x\text{MnO}_3$ as a function of x as shown in Figure 4. The μ_{AF} and μ_{FM} represent the average AF and FM magnetic moments. The changeover from AF to FM region for increasing x in our case is gradual, but in the real experiment for $\text{La}_{1-x}\text{Ca}_x\text{MnO}_3$, it is very sharp. This crossover takes place at $x \sim 0.16$ and $x \sim 0.082$ for the $\text{La}_{1-x}\text{Ca}_x\text{MnO}_3$ and for the $\text{La}_{1-x}\text{Sr}_x\text{MnO}_3$ respectively. Such different behavior can be understood on the basis of the distinct ionic radius [22] and electron affinity [23] of the alkaline ions. In particular, the FM moments are progressively reduced as the radius of lanthanide is shortened. Since the radius of Sr^{2+} ions is greater than that of Ca^{2+} ions, the FM frustration is enhanced in the Sr-based Mn-oxides at a smaller x than that of the Ca-based Mn-oxides. Although the exact description of the magnetic frustration at present is not clear, it may originate from the enhancement of the effective AF coupling [21]. However, our result of $S(q)$ is at least qualitatively well compared with experiments.

Now let us look at the PS from a snapshot of the localized spins configuration. The spatial dependence of the azimuthal angle of the local spins $S_i^z = \cos(\theta_i)$ is plotted in Figure 5. The average density of the conduction electron is $\langle n \rangle = 0.886$. The coexistence of the AF and FM portions is clearly seen. These two magnetic states strongly depends on the density of conduction electrons. At high electron density, the low conducting FM phase is embedded in an insulating AF host, resulting in globally

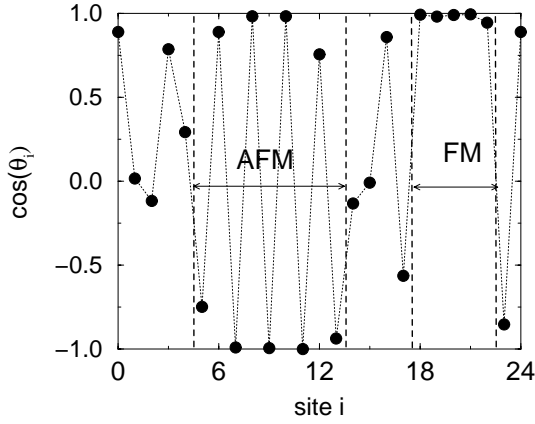


Fig. 5. Spatial dependence of the azimuthal angle θ_i of the t_{2g} spin \mathbf{S}_i for $J_H = 12t$, $T = t/80$ and $\mu = -10.5497$. The average hole density is closed to $x \approx 0.114$.

low conductivity. But, as the hole carrier density increases, the phase segregation occurs from the low conducting AF to high conducting FM region. Thus, one sees that the hole-poor region is an insulating AF while the hole-rich region is a conducting FM state. From this analysis, we observed that the coexistence of the hole-poor AF and hole-rich FM portion is intrinsic in the FM Kondo lattice model.

Indeed a large number of experimental papers [8–11] have reported the presence of the phase separation in the doped manganites, and our study seem to be in qualitative agreement with experiments. However, as demonstrated in the recent works [17,18], the superexchange interactions among t_{2g} local spins, in addition to the strong Hund coupling, play an important role in determination of the phase separation. Further, Yunoki *et al.* [24] pointed out that the phase separation is also induced by the orbital degree of freedom for large electron-phonon coupling, which means that one has to take account of both the superexchange interactions and the Jahn-Teller effects for the proper description of Mn-oxides. Despite the basic differences between 1-orbital and 2-orbital with JT phonons, the phase separation tendencies are similar to the phenomenon observed in our scheme. It suggests that the interplay of the local FM spin alignment induced by conduction electrons *via* double exchange mechanism is a crucial ingredient. But, further studies are required to clarify the nature of the phase separation in doped manganites.

In conclusion, the PS of the FM Kondo lattice model is clearly demonstrated by the direct observation of a snapshot of spin configuration. The evidences of the density of states, density fluctuation as well as spin-spin correlations also support this result. At a fixed density, magnetic regions are separated spatially into the hole-poor AF and the hole-rich FM phase. In the phase separation region, the doping dependence of the spin structure factors is presented and compared with experiments.

We are grateful to Prof. Soonchil Lee and Drs. Kihoon Kim and Jinhyoung Lee for helpful discussions. This work was

supported by the Korea Science Engineering Foundation (95-0702-03-01-3) and by the Basic Science Research Institute program, Ministry of Education, 1997, Project No. 97-2415. Additional support was provided by Creative Research Initiatives of the Korean Ministry of Science and Technology. A part of the present calculations was performed on the JRCAT Supercomputer System, which is supported by New Energy and Industrial Technology Development Organization (NEDO) of Japan.

References

1. For a review see, A.P. Ramirez, J. Phys.-Cond. **9**, 8171 (1997).
2. P. Schiffer, A.P. Ramirez, W. Bao, S.-W. Cheong, Phys. Rev. Lett. **75**, 3336 (1995); P.G. Radaelli, D.E. Cox, M. Marezio, S.-W. Cheong, P.E. Schiffer, A.P. Ramirez, Phys. Rev. Lett. **75**, 4488 (1995).
3. C. Zener, Phys. Rev. **82**, 403 (1951); J.B Goodenough, Phys. Rev. **100**, 565 (1955); P.W. Anderson, H. Hasegawa, Phys. Rev. **100**, 675 (1955); K. Kubo, N. Ohata, J. Phys. Soc. Jpn **33**, 21 (1972).
4. P.G. de Gennes, Phys. Rev. **118**, 141 (1960).
5. E. Wollan, W. Koehler, Phys. Rev. **100**, 545 (1955).
6. H. Kawano, R. Kajimoto, M. Kubota, H. Yoshizawa, Phys. Rev. B **53**, 2202 (1996).
7. G. Matsumoto, J. Phys. Soc. Jpn **29**, 606 (1970); *ibid.* **29**, 615 (1970).
8. M. Hennion, F. Moussa, J. Rodriguez-Carvajal, L. Ponsard, A. Revcolevschi, Phys. Rev. B **56**, R498 (1997).
9. M. Hennion, F. Moussa, G. Biotteau, J. Rodriguez-Carvajal, L. Ponsard, A. Revcolevschi, Phys. Rev. Lett. **81**, 1957 (1997).
10. G. Allodi, R. De Renzi, G. Guidi, F. Licci, M.W. Pieper, Phys. Rev. B **56**, 6036 (1997).
11. G. Allodi, R. De Renzi, G. Guidi, Phys. Rev. B **57**, 1024 (1998).
12. V.J. Emery, S.A. Kivelson, H.Q. Lin, Phys. Rev. Lett. **64**, 475 (1990); V.J. Emery, S.A. Kivelson, Physica C **209**, 597 (1993); U. Löw, V.J. Emery, K. Fabricius, S.A. Kivelson, Phys. Rev. Lett. **72**, 1918 (1994).
13. E.L. Nagaev, Phys. Stat. Sol. (b) **186**, 9 (1994).
14. D.P. Arovas, F. Guinea, Phys. Rev. B **58**, 9150, (1998).
15. M. Kagan, K. Khomskii, M. Mostovoy, cond-mat/9804213.
16. S. Yunoki, J. Hu, A. Malvezzi, A. Moreo, N. Furukawa, E. Dagotto, Phys. Rev. Lett. **80**, 845 (1998); E. Dagotto, S. Yunoki, A. Malvezzi, A. Moreo, J. Hu, S. Capponi, D. Poilblanc, N. Furukawa, Phys. Rev. B **58**, 6414 (1998).
17. S. Yunoki, A. Moreo, Phys. Rev. B **58**, 6403 (1998).
18. Hongsuk Yi, Jaejun Yu, Phys. Rev. B **58**, 11123 (1998).
19. The value of the finite energy interval is ($\Delta\omega = 0.3$).
20. J. Inoue, S. Maekawa, Phys. Rev. Lett. **74**, 3407 (1995).
21. Hongsuk Yi, Jaejun Yu, Sung-Ik Lee (unpublished).
22. H.Y. Hwang, S.-W. Cheong, P.G. Radaelli, M. Marezio, B. Batlogg, Phys. Rev. Lett. **75**, 914 (1995).
23. J.L. Garcia-Muñoz, J. Fontcuberta, B. Martinez, A. Seffar, S. Piñol, X. Obradors, Phys. Rev. B **55**, R668 (1997).
24. S. Yunoki, A. Moreo, E. Dagotto, Phys. Rev. Lett. **81**, 5612 (1998); E. Dagotto, S. Yunoki, A. Moreo, cond-mat/9809380.